

Sc_{0.43(2)}Rb₂Mo₁₅S₁₉, a partially Sc-filled variant of Rb₂Mo₁₅S₁₉

Patrick Gougeon,^{a*} Rabih Al Rahal Al Orabi,^a Régis Gautier^b and Michel Potel^a

^aSciences Chimiques de Rennes, CSM–INSA, UMR CNRS No. 6226, Université de Rennes I, Avenue du Général Leclerc, 35042 Rennes CEDEX, France, and ^bSciences Chimiques de Rennes, UMR CNRS 6226, Ecole Nationale Supérieure de Chimie de Rennes, Avenue du Général Leclerc, CS 50837, 35708 Rennes CEDEX 7, France
Correspondence e-mail: patrick.gougeon@univ-rennes1.fr

Received 29 March 2012

Accepted 16 April 2012

Online 25 April 2012

The structure of scandium dirubidium pentadecamolybdenum nonadecasulfide, Sc_{0.43(2)}Rb₂Mo₁₅S₁₉, constitutes a partially Sc-filled variant of Rb₂Mo₁₅S₁₉ [Picard, Saillard, Gougeon, Noel & Potel (2000), *J. Solid State Chem.* **155**, 417–426]. In the two compounds, which both crystallize in the $R\bar{3}c$ space group, the structural motif is characterized by a mixture of Mo₆S₈S₆ⁱ and Mo₉S₁₁S₆^a cluster units ('i' is inner and 'a' is apical) in a 1:1 ratio. The two components are interconnected through interunit Mo–S bonds. The cluster units are centred at Wyckoff positions *6b* and *6a* (point-group symmetries $\bar{3}$. and 32 , respectively). The Rb⁺ cations occupy large voids between the different cluster units. The Rb and the two inner S atoms lie on sites with 3. symmetry (Wyckoff site 12c), and the Mo and S atoms of the median plane of the Mo₉S₁₁S₆ cluster unit lie on sites with .2 symmetry (Wyckoff site 18e). A unique feature of the structure is a partially filled octahedral Sc site with $\bar{1}$ symmetry. Extended Hückel tight-binding calculations provide an understanding of the variation in the Mo–Mo distances within the Mo clusters induced by the increase in the cationic charge transfer due to the insertion of Sc.

Comment

In₂Mo₁₅Se₁₉ (Potel *et al.*, 1981) and In₃Mo₁₅Se₁₉ (Grüttner *et al.*, 1979), which crystallize in the $R\bar{3}c$ and $P6_3/m$ space groups, respectively, were the first compounds containing a molybdenum cluster with a nuclearity greater than 6. Indeed, their crystal structures contain an equal mixture of octahedral Mo₆ and bioctahedral Mo₉ clusters. Subsequently, compounds isotopic with In₂Mo₁₅Se₁₉, such as Al₂Mo₁₅S₁₉ (Alc = K, Rb or Cs; Picard *et al.*, 2002, 2000, 2004) or Ba₂Mo₁₅Se₁₉ (Gougeon *et al.*, 1989), as well as compounds isotopic with In₃Mo₁₅Se₁₉, such as In_{1.6}Rb₂Mo₁₅S₁₉ and ScTi₂Mo₁₅S₁₉ (Salloum *et al.*, 2004), have been obtained. Among the latter compounds, Rb₂Mo₁₅S₁₉ appears to be the first member of the series of compounds Rb_{2n}Mo₉S₁₁Mo_{6n}S_{6n+2} ($n = 1, 2, 3$ and 4 ;

Picard *et al.*, 2000). In addition to their interesting crystal structures, the Rb_{2n}Mo₉S₁₁Mo_{6n}S_{6n+2} compounds become superconducting at low temperature. In an attempt to replace Tl with Rb in ScTi₂Mo₁₅Se₁₉ (In₃Mo₁₅Se₁₉ type), we obtained the title new quaternary compound Sc_{0.43}Rb₂Mo₁₅S₁₉ belonging to the In₂Mo₁₅Se₁₉ structure type and constituting a partially Sc-filled variant of Rb₂Mo₁₅S₁₉.

The insertion of Sc into Rb₂Mo₁₅S₁₉ is evident from the variations in the unit-cell parameters: the *a* axis increases by *ca* 0.08 Å, while the *c* axis decreases by about 0.27 Å. A view of the crystal structure of Sc_{0.43}Rb₂Mo₁₅S₁₉ is shown in Fig. 1. The Mo–S framework is similar to that of Rb₂Mo₁₅S₁₉ and is based on an equal mixture of Mo₆S₈S₆ⁱ and Mo₉S₁₁S₆^a cluster units interconnected through Mo–S bonds (Fig. 2) [for details of the inner ('i') and apical ('a') ligand notation, see Schäfer & von Schnering (1964)]. The first unit can be described as an Mo₆ octahedron surrounded by eight face-capping inner Sⁱ (six S3 and two S5) and six apical S^a (S1) ligands. The Mo₉ core of the second unit results from the face-sharing of two octahedral Mo₆ clusters. The Mo₉ cluster is surrounded by 11 Sⁱ atoms (six S1, three S2 and two S4) capping the faces of the bioctahedron and six apical S^a ligands (S3) above the outer Mo atoms. The Mo₆S₈S₆ⁱ and Mo₉S₁₁S₆^a units are centred at the *6b* and *6a*

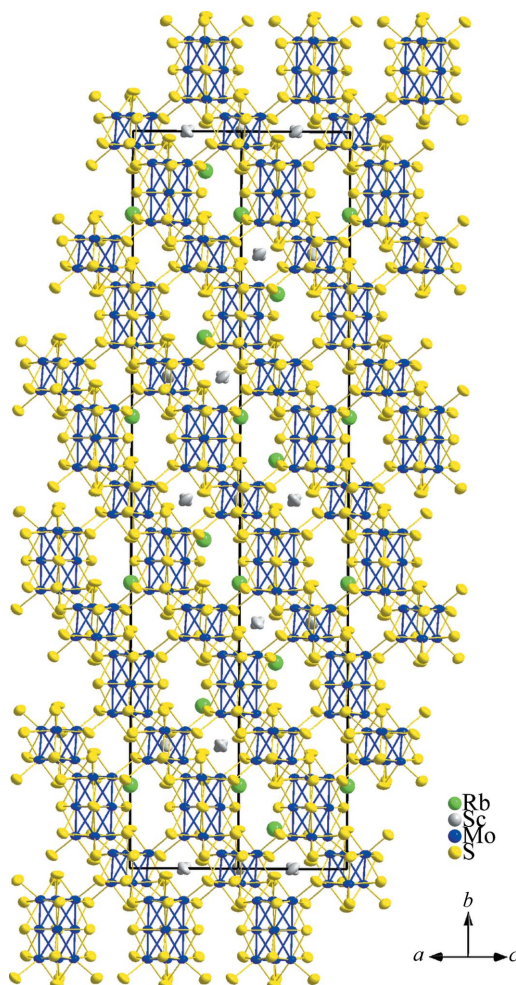


Figure 1
A view of Sc_{0.43}Rb₂Mo₁₅S₁₉ along [110].

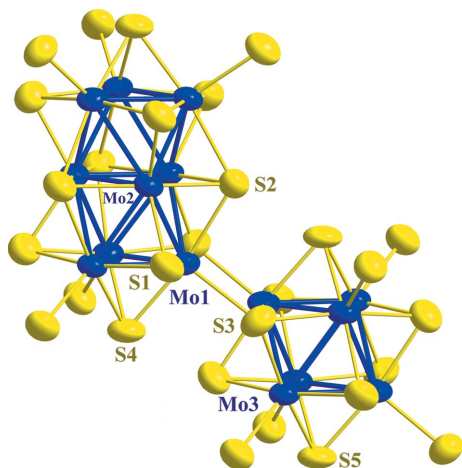


Figure 2

A plot showing the atom-numbering scheme and the inter-unit linkage of the $\text{Mo}_9\text{S}_{11}\text{S}_6$ and $\text{Mo}_6\text{S}_8\text{S}_6$ cluster units. Displacement ellipsoids are drawn at the 97% probability level.

positions and have point-group symmetries $\bar{3}$ and 32, respectively.

The Mo–Mo distances within the Mo_6 clusters are 2.6783 (6) Å for the intratriangle distances (distances within the Mo_3 triangles formed by atoms Mo3 related through the threefold axis) and 2.7393 (6) Å for the intertriangle distances. In $\text{Rb}_2\text{Mo}_{15}\text{S}_{19}$, the latter two values are 2.676 (2) and 2.767 (2) Å, respectively. These variations reflect the different cationic charge transfer towards the Mo_6 clusters in the two parent compounds.

The Mo–Mo distances within the Mo_9 clusters are 2.6658 (5) and 2.6910 (8) Å for the distances in the triangles formed by atoms Mo1 and Mo2, respectively. In $\text{Rb}_2\text{Mo}_{15}\text{S}_{19}$, the corresponding distances are 2.680 (2) and 2.688 (3) Å. The distances between the triangles formed by atoms Mo1 and Mo2 are 2.6958 (4) and 2.7663 (4) Å, respectively, in $\text{Sc}_{0.43}\text{Rb}_2\text{Mo}_{15}\text{S}_{19}$, compared with 2.719 (1) and 2.785 (2) Å, respectively, in $\text{Rb}_2\text{Mo}_{15}\text{S}_{19}$.

Although the structural response of the Mo_9 cluster with respect to the increase in charge transfer is more complex, we observe that the Mo1–Mo1 and two Mo1–Mo2 intertriangle distances are shorter in the Sc-filled compound. On the other hand, a slight increase in the Mo2–Mo2 bond distances occurs in the median Mo_3 triangle [2.688 (3) Å in $\text{Rb}_2\text{Mo}_{15}\text{S}_{19}$]. In order to explain these variations, we performed extended Hückel tight-binding (EHTB) calculations on $\text{Rb}_2\text{Mo}_{15}\text{S}_{19}$ using the program *YaEHMOP* (Landrum, 1997). The Mo and S extended Hückel parameters used by Picard *et al.* (2000) were considered. Total Mo_6 - and Mo_9 -projected DOS (density of states) and COOP (crystal orbital overlap population) curves for the different bonds discussed above and obtained from 36 k points of the irreducible wedge of the Brillouin zone are sketched in Figs. 3 and 4, respectively.

Assuming an ionic interaction between the inserted Sc atoms and the host material, the three electrons of the 3d transition metal should be transferred to the clusters.

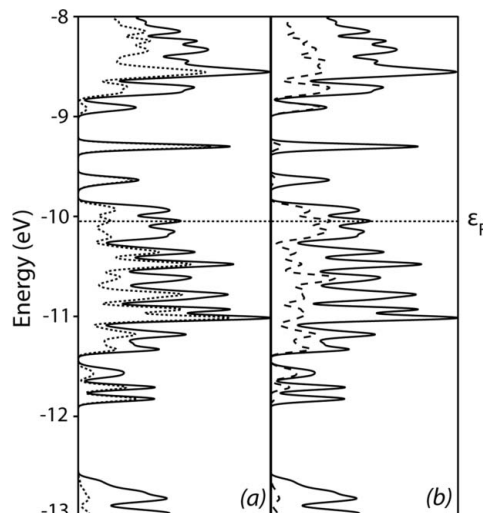


Figure 3

EHTB calculations for $\text{Rb}_2\text{Mo}_{15}\text{S}_{19}$, showing (a) total (solid line) and Mo_6 -projected (dotted line) DOS, and (b) total (solid line) and Mo_9 -projected (dotted line) DOS.

Assuming a rigid-band model, the Fermi level corresponding to the electron count of the title compound is slightly higher in energy (*ca.* 0.02 eV) than that for $\text{Rb}_2\text{Mo}_{15}\text{S}_{19}$. The DOS at the Fermi level is mainly centred on Mo atoms belonging to both Mo_6 and Mo_9 clusters (Fig. 3). Therefore, both clusters should be affected by an increase in the anionic charge of the Mo–S network. As shown by the COOP curves of the Mo3–Mo3 intratriangle (solid line) and Mo3–Mo3 intertriangle (dotted line) bonds within the Mo_6 cluster, the increase in the metal electron count due to the insertion of Sc foresees a weak lengthening and a shortening of the Mo3–Mo3 bonds within the Mo_3 triangles and between the triangles, respectively. Such an evolution is in fact observed in $\text{Sc}_{0.4}\text{Rb}_2\text{Mo}_{15}\text{S}_{19}$, as mentioned above.

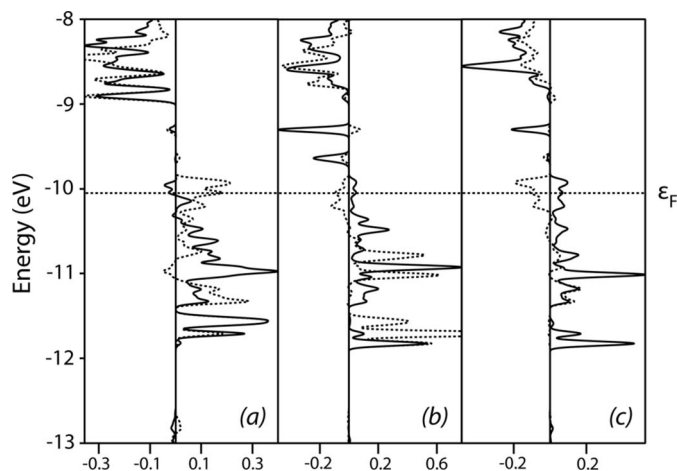


Figure 4

EHTB calculations for $\text{Rb}_2\text{Mo}_{15}\text{S}_{19}$, showing (a) Mo3–Mo3 COOPs for intratriangle (solid line) and intertriangle (dotted line) bonds of the Mo_6 cluster, (b) COOPs for the intratriangle Mo1–Mo1 (solid line) and Mo2–Mo2 (dotted line) bonds in the Mo_9 cluster and (c) COOPs for the intertriangle Mo1–Mo2 bonds of 2.719 (solid line) and 2.785 Å (dotted line).

Intensity data were collected on the Nonius KappaCCD X-ray diffractometer system of the 'Centre de diffractométrie de l'Université de Rennes I' (<http://www.cdifx.univ-rennes1.fr>).

Supplementary data for this paper are available from the IUCr electronic archives (Reference: FN3104). Services for accessing these data are described at the back of the journal.

References

- Altomare, A., Burla, M. C., Camalli, M., Cascarano, G. L., Giacovazzo, C., Guagliardi, A., Moliterni, A. G. G., Polidori, G. & Spagna, R. (1999). *J. Appl. Cryst.* **32**, 115–119.
- Brandenburg, K. (1996). *DIAMOND*. University of Bonn, Germany.
- Duisenberg, A. J. M., Kroon-Batenburg, L. M. J. & Schreurs, A. M. M. (2003). *J. Appl. Cryst.* **36**, 220–229.
- Gougeon, P., Potel, M. & Sergent, M. (1989). *Acta Cryst.* **C45**, 1285–1287.
- Grüttner, A., Yvon, K., Chevrel, R., Potel, M., Sergent, M. & Seeber, B. (1979). *Acta Cryst.* **B35**, 285–292.
- Landrum, G. A. (1997). *YAeHMOP (Yet Another Extended Hückel Molecular Orbital Package)*. Cornell University, Ithaca, New York, USA.
- Liang, Z.-H., Tang, K.-B., Chen, Q.-W. & Zheng, H.-G. (2009). *Acta Cryst.* **E65**, i44.
- Meulenaer, J. de & Tompa, H. (1965). *Acta Cryst.* **19**, 1014–1018.
- Nonius (1998). *COLLECT*. Nonius BV, Delft, The Netherlands.
- Picard, S., Gougeon, P. & Potel, M. (2002). *Acta Cryst.* **E58**, i12–i14.
- Picard, S., Saillard, J.-Y., Gougeon, P., Noel, H. & Potel, M. (2000). *J. Solid State Chem.* **155**, 417–426.
- Picard, S., Salloum, D., Gougeon, P. & Potel, M. (2004). *Acta Cryst.* **C60**, i61–i62.
- Potel, M., Chevrel, R. & Sergent, M. (1981). *Acta Cryst.* **B37**, 1007–1010.
- Salloum, D., Gougeon, P., Roisnel, T. & Potel, M. (2004). *J. Alloys Compd.* **383**, 57–62.
- Schäfer, H. & von Schnering, H. G. (1964). *Angew. Chem.* **76**, 833–845.
- Sheldrick, G. M. (2008). *Acta Cryst.* **A64**, 112–122.
- Solodovnikova, Z. A. & Solodovnikov, S. F. (2006). *Acta Cryst.* **C62**, i53–i56.
- Zhao, D., Li, F. F., Qiu, S., Jiao, J. & Ren, J. (2011). *Acta Cryst.* **E67**, i32.